GENERALIZED BLIND MISMATCH CORRECTION FOR TWO-CHANNEL TIME-INTERLEAVED A-TO-D CONVERTERS

Munkyo Seo, Mark Rodwell, Upamanyu Madhow

Department of Electrical and Computer Engineering
University of California, Santa Barbara
Santa Barbara, CA 93106 USA

ABSTRACT

Calibration of sub-converter mismatches is a challenging task for high-performance time-interleaved analog-to-digital converters (TIADC). Presently known blind correction methods can remove static gain and sampling time mismatches. However, actual sub-converters significantly deviate from a simple gain-timing model, and the resulting modeling error strictly limits maximum output signal-to-noise ratio achievable. Generalized mismatch modeling is, therefore, necessary to break the limitation of gain-timing model. In this paper, we propose a blind method for correcting generalized mismatch errors for M=2 TIADC, which is the first in the literature to the authors' knowledge. Cyclostationary spectral analysis shows that unique identification is possible in most practical cases. Simulation results show significant performance improvement by the proposed generalized correction method.

Index Terms— analog-digital conversion, calibration, time-interleaved, adaptive equalizers, adaptive signal processing.

1. INTRODUCTION

A time-interleaved analog-to-digital converter (TIADC) has a parallel structure where a number of sub-converters cyclically sample the input signal, and outputs are similarly taken to form a digital stream. The overall sampling rate linearly increases with the number of sub-converters, and therefore a TIADC is suited for high-speed analog-digital (A/D) conversion systems [1].

It is well known that the spectral performance of a TIADC is seriously degraded by sub-converter mismatches. Such mismatches create noise sidebands by modulating the input, and eventually limit the output signal-to-noise ratio (SNR) or spur-free dynamic range (SFDR). Mismatches can be digitally corrected by either training [5] or blind methods [2]-[4], [6]-[7]. Training methods are suitable for high-resolution applications since they are capable of correcting general linear mismatches, but at the cost of system suspension during each calibration. Blind methods allow uninterrupted system operation and can track slowly time-varying errors, but currently known blind methods can only handle static gain and timing mismatches.

The calibration performance of this gain-timing correction depends on specific converter hardware and the input signal bandwidth. If the TIADC input circuitry and sub-converters have high enough bandwidth with no in-band poles or zeros, then the static gain and time delay may adequately model a sub-converter. If, however, the lowest input pole (or zero) is not sufficiently higher than the input bandwidth, the gain and phase response is no longer a straight line. As a result, mismatches in the location of pole (or zero) between channels will produce nonlinear gain and phase mismatch response. If the input circuitry has a bandpass nature, the displacement of lower-frequency poles (or zeros) will also result complicated mismatch behavior [5]. This modeling error is irreducible and acts as residual mismatches, making gain-timing model inadequate for high-resolution applications. The effect of such under-modeled mismatches is more serious with wideband input signals [7].

It is clear at this point that generalized mismatch correction is necessary to break the limitation of simple gain-timing model for a higher level of calibration performance. Now, the challenge is how to handle the increased number of estimation parameters resulting from *generalizing* correctible mismatches. The blind search algorithm will more likely end up at local minima, resulting *false correction*. The pertinent goal is to find a combination of realistic constraints and mismatch parameterization such that the blind algorithm can uniquely identify a necessary number of mismatch parameters under most practical cases. Our blind method is based on polynomial mismatch approximation and wide-sense stationary (WSS) input assumption. The WSS input assumption is mainly for theoretical purpose, however, and in practice the proposed method works with most stochastically non-WSS signals as well. We will show that this particular combination enables multi-parameter estimation and eliminates false correction in most practical cases.

2. SYSTEM CONFIGURATION

A two-channel TIADC system is shown in Fig.1 (a). The sample period and frequency of the array is T_s and $\omega_s=2\pi/T_s$, respectively. The analog input $x(t)$ is bandlimited from dc to $0.5\omega_s$, and assumed to be a real-valued, zero-mean and WSS random process. Fig.1 (b) illustrates a linear equivalent model with channel transfer function (CTF) $H_0(\omega)$ and $H_1(\omega)$. Any linear filtering effects before A/D conversion are lumped into the CTF, including static gain, sampling time shift, pole-zero effect, etc. Assuming the bit-resolution is high, quantization effects are ignored. Normalization with respect to the first channel yields Fig.1 (c), where the correction digital filters $F_0(e^{j\omega})$ and $F_1(e^{j\omega})$ are also shown. This normalization clarifies we are interested only in channel *mismatches*, disregarding common linear time-invariant (LTI) filtering. There are two justifications for this: first, the LTI system does not create distortion sidebands, and second, common filtering due to CTF is acceptable in most cases. Now, the normalized CTF

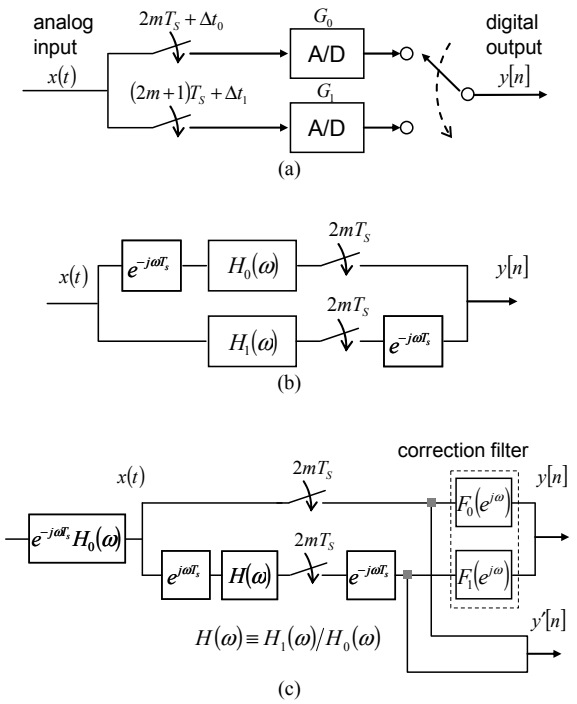

Figure 1. M=2 TIADC system model: (a) physical system, (b) equivalent system and (c) normalized system with correction filter bank. $y[n]$ and $y'[n]$ is corrected and uncorrected output, respectively.

$H(\omega)\equiv H_1(\omega)/H_0(\omega)$ fully characterizes the general linear mismatches between the two channels.

The system in Fig.1 (c) can be regarded as an M=2 filter bank, with analysis and synthesis filter bank equal to the analog and digital filters, respectively. The alias component (AC) matrix for each bank is then defined as [8]

$$\mathbf{H}_{\mathbf{AC}}(\omega,\mathbf{p}_0)=\begin{pmatrix}1 & H(\omega)\\ 1 & -H(\omega-\omega_s/2)\end{pmatrix}\begin{pmatrix}1 & 0\\ 0 & e^{j\omega T_s}\end{pmatrix}, \quad (1)$$

$$\mathbf{F}_{\mathbf{AC}}(e^{j\omega},\tilde{\mathbf{p}})=\begin{pmatrix}F_0(e^{j\omega}) & F_1(e^{j\omega})\\ F_0(e^{j(\omega-\omega_s/2)}) & -F_1(e^{j(\omega-\omega_s/2)})\end{pmatrix}\begin{pmatrix}1 & 0\\ 0 & e^{-j\omega T_s}\end{pmatrix}.$$

Note that $\mathbf{H}_{\mathbf{AC}}$ and $\mathbf{F}_{\mathbf{AC}}$ is a function of $\mathbf{p}_0$ and $\tilde{\mathbf{p}}$ which is an actual and estimated mismatch parameter vector, respectively. The perfect reconstruction condition is [8]

$$\mathbf{H}_{\mathbf{AC}}\mathbf{F}_{\mathbf{AC}}^{\mathbf{T}}=2\mathbf{I}, \quad (2)$$

which means that the entire system in Fig.1 (c) reduces to an LTI system with no aliasing error. Equation (2) suggests that the correction filter should be designed as

$$\mathbf{F}_{\mathbf{AC}}(e^{j\omega},\tilde{\mathbf{p}})=2\tilde{\mathbf{H}}_{\mathbf{AC}}^{-\mathbf{T}}(\omega,\tilde{\mathbf{p}}), \quad (3)$$

where $\tilde{\mathbf{H}}_{\mathbf{AC}}$ is the AC matrix of a hypothetical analysis filter bank (assumed to be invertible),

$$\tilde{\mathbf{H}}_{\mathbf{AC}}(\omega,\tilde{\mathbf{p}})=\begin{pmatrix}1 & \tilde{H}(\omega)\\ 1 & -\tilde{H}(\omega-\omega_s/2)\end{pmatrix}\begin{pmatrix}1 & 0\\ 0 & e^{j\omega T_s}\end{pmatrix}. \quad (4)$$

$\tilde{H}(\omega)$ is the estimated CTF parameterized by mismatch estimation $\tilde{\mathbf{p}}$. The correction filters can be designed as follows: First, specify $\tilde{H}(\omega)$ using the current estimation $\tilde{\mathbf{p}}$, second, build $\tilde{\mathbf{H}}_{\mathbf{AC}}$ using (4), third, invert it to obtain $\mathbf{F}_{\mathbf{AC}}$ using (3), and finally obtain the time-domain impulse response using any conventional filter design method (e.g. frequency sampling, least-squares, etc).

$$\begin{aligned} f_0[n]&=\mathrm{IDFT}\left(F_0(e^{j\omega})\right),\\ f_1[n]&=\mathrm{IDFT}\left(F_1(e^{j\omega})\right). \end{aligned} \quad (5)$$

In (5), IDFT(·) is the inverse discrete Fourier transform operator. $f_0[n]$'s and $f_1[n]$'s are correction filter taps, whose combined output is the mismatch-corrected TIADC output in Fig.1 (c).

3. CYCLOSTATIONARITY CHARACTERIZATION

A TIADC is a periodically time-varying linear system. Given a WSS input, the output is wide-sense cyclostationary (WSCS). If there is no mismatch, the output is also WSS. The proposed blind method seeks to the following input-output WSS condition: *assuming a WSS input, adjust the correction filter such that the TIADC output restores WSS property*. For an M=2 TIADC with gain-timing model, the attainment of output WSS condition was shown to be necessary and sufficient for actual mismatch correction under input WSS assumption [6]. This WSS-based framework also proves useful for generalized mismatch model. The characterization of WSCS processes in this paper follows the convention in [9]. Note that the proposed algorithm is equally valid with most practical signals not WSS in a stochastic sense. In reality, we rely on time-averaging (rather than *stochastic* expectation) to get the empirical autocorrelation, and therefore non-stationary part of the input will be effectively smoothed out, unless the input signal has exact phase relationships with the sampling clock (e.g. $\sin(\pi(m/M)f_s t)$, m=1,…,M-1 where M is the number of TIADC channels).

The autocorrelation function of the TIADC output $y[n]$ is given by $R_y[n,n']\equiv E[y[n]y[n']]$. A random process is called WSCS if its autocorrelation is periodic with respect to the common shift. Note that WSS processes are also WSCS, but not vice versa. The TIADC output autocorrelation R_y then satisfies (for M=2),

$$R_y[n,n']=R_y[n+2,n'+2] \quad \text{for all } n,n'. \quad (6)$$

If channel mismatch is present, R_y is in general (but not necessarily) shift-dependent,

$$R_y[n,n']\neq R_y[n+1,n'+1] \quad \text{for all } n,n'. \quad (7)$$

If no mismatch, $y[n]$ is WSS and R_y is always shift-independent.

$$R_y[n,n']=R_y[n+1,n'+1] \quad \text{for all } n,n'. \quad (8)$$

From (6)-(8), it is readily seen that R_y is completely specified by $R_y[u,0]$ and $R_y[u+1,1]$ for all u. Another equivalent representation is the so called cyclic correlation function, which is defined as a Fourier series coefficient of $R_y[n,n']$. For M=2, it is a simple sum or difference,

$$\begin{aligned} R_y^0[u]&=\frac{1}{2}\left(R_y[u,0]+R_y[u+1,1]\right),\\ R_y^{1/2}[u]&=\frac{1}{2}\left(R_y[u,0]-R_y[u+1,1]\right). \end{aligned} \quad (9)$$

Taking Fourier transform of (9), we obtain cyclic spectral density (CSD),

$$S_y^{\alpha}(\omega)=\sum_{u=-\infty}^{+\infty}R_y^{\alpha}[u]e^{-j\omega u}\quad \alpha\in\left\{0,\frac{1}{2}\right\}. \tag{10}$$

Note that $R_y^{1/2}[u]\equiv 0$ and $S_y^{1/2}(\omega)\equiv 0$ for WSS $y[n]$. In this case, $R_y^{0}[u]$ and $S_y^{0}(\omega)$ reduces to the conventional autocorrelation and spectral density of WSS processes, respectively. Thus, $R_y^{1/2}[u]$ or $S_y^{1/2}(\omega)$ provides a measure of how close $y[n]$ is to being WSS. The following definition of CSD matrix is useful for TIADC spectral analysis.

$$\mathbf{S_Y}(\omega)\equiv\begin{pmatrix} S_y^{0}(\omega) & S_y^{1/2}(\omega) \\ S_y^{1/2^*}(\omega-\omega_s/2) & S_y^{0}(\omega-\omega_s/2)\end{pmatrix}. \tag{11}$$

It immediately follows that $\mathbf{S_Y}(\omega)$ becomes a diagonal matrix for WSS $y[n]$. Let $\mathbf{S_X}(\omega)$ be the diagonal CSD matrix for the WSS TIADC input $x[n]\equiv x(nT_s)$. It can be shown that $\mathbf{S_Y}(\omega)$ has the following relationship with $\mathbf{S_X}(\omega)$ [9].

$$\begin{aligned}\mathbf{S_Y}(\omega)&=(1/4)\left(\mathbf{F_{AC}}\mathbf{H_{AC}^{T}}\right)\mathbf{S_X}(\omega)\left(\mathbf{F_{AC}}\mathbf{H_{AC}^{T}}\right)^{\mathbf{H}}\\&=\left(\tilde{\mathbf{H}}_{\mathbf{AC}}^{-\mathbf{T}}\mathbf{H_{AC}^{T}}\right)\mathbf{S_X}(\omega)\left(\tilde{\mathbf{H}}_{\mathbf{AC}}^{-\mathbf{T}}\mathbf{H_{AC}^{T}}\right)^{\mathbf{H}}.\end{aligned} \tag{12}$$

4. ALGORITHM DESCRIPTION

Following the previous discussion, we can achieve the input-output WSS condition by minimizing the norm of $R_y^{1/2}[u]$,

$$\tilde{\mathbf{p}}_{opt}=\arg\min_{\tilde{\mathbf{p}}}\sum_{u=0}^{U_{\max}}\left(R_y^{1/2}[u]\right)^2, \tag{13}$$

where $\tilde{\mathbf{p}}_{\text{opt}}$ is the best estimation of mismatch parameters, and U_{max} is the maximum time lag to consider. We have yet to answer an important question: Under which conditions does the input-output WSS actually guarantee that $\tilde{\mathbf{p}}_{\text{opt}}=\mathbf{p}_0$? We begin with $S_y^{1/2}(\omega)$, Fourier transform of $R_y^{1/2}[u]$. From (11) and (12), it is written as

$$\begin{aligned}S_y^{1/2}(\omega)=&S_x^{0}(\omega)\left(\tilde{H}^{*}(\omega)-H^{*}(\omega)\right)\left(H(\omega)+\tilde{H}(\omega-\omega_s/2)\right)\\&+S_x^{0}(\omega-\omega_s/2)\left(\tilde{H}(\omega-\omega_s/2)-H(\omega-\omega_s/2)\right)\\&\cdot\left(\tilde{H}^{*}(\omega)+H^{*}(\omega-\omega_s/2)\right)\end{aligned}. \tag{14}$$

We rewrite CTF's in a polar form, and apply small-mismatch assumption to yield

$$\begin{aligned}H(\omega)&=\left(1+g(\omega)\right)e^{j\phi(\omega)}\approx 1+g(\omega)+j\phi(\omega)\\\tilde{H}(\omega)&=\left(1+\tilde{g}(\omega)\right)e^{j\tilde{\phi}(\omega)}\approx 1+\tilde{g}(\omega)+j\tilde{\phi}(\omega)\end{aligned}. \tag{15}$$

Representing each error term in (15) as a Q-th order polynomial, we have

$$\begin{aligned}g(\omega)&=\sum_{k=0}^{Q}a_k\omega^k,\quad \phi(\omega)=\sum_{k=0}^{Q}b_k\omega^k,\\\tilde{g}(\omega)&=\sum_{k=0}^{Q}\tilde{a}_k\omega^k,\quad \tilde{\phi}(\omega)=\sum_{k=0}^{Q}\tilde{b}_k\omega^k.\end{aligned} \tag{16}$$

Thus, $\mathbf{p}_0=(a_0\ a_1\ \dots\ a_Q\ b_0\ b_1\ \dots\ b_Q)^{\mathrm{T}}$ and $\tilde{\mathbf{p}}=(\tilde{a}_0\ \tilde{a}_1\ \dots\ \tilde{a}_Q\ \tilde{b}_0\ \tilde{b}_1\ \dots\ \tilde{b}_Q)^{\mathrm{T}}$. Plugging (15)-(16) into (14), and taking real and imaginary part, we can show that, to a first-order approximation, $S_y^{1/2}(\omega)\equiv 0$ is equivalent to the following matrix-vector equations.

$$\begin{aligned}\mathbf{W}\mathbf{e_g}&=\mathbf{0},\\\mathbf{W}\mathbf{e_\varphi}&=\mathbf{0},\end{aligned} \tag{17}$$

where $\mathbf{W}$ and coefficient error vectors $\mathbf{e}_{\mathrm{g}}$ and $\mathbf{e}_{\varphi}$ are defined as

$$\begin{aligned}&\left[\mathbf{W}\right]_{n,m}=S_y^{0}(\omega_n)\omega_n^m+S_y^{0}(\omega_n-\omega_s/2)(\omega_s/2-\omega_n)^m,\\&\left[\mathbf{e_g}\right]_{n,1}=\tilde{a}_n-a_n,\\&\left[\mathbf{e_\varphi}\right]_{n,1}=\tilde{b}_n-b_n.\\&\left(0\le n\le F-1,\ 0\le m\le Q,\ 0<\omega_n<\omega_s/2\right)\end{aligned}. \tag{18}$$

ω_n's are F frequency points where either $S_y^{0}(\omega_n)$ or $S_y^{0}(\omega_n-\omega_s/2)$ is nonzero (hence positive). If $\mathbf{W}$ has at least $(Q+1)$ linearly independent rows, then the only solution of (17) is $\mathbf{e}_{\mathrm{g}}=\mathbf{0}$ and $\mathbf{e}_{\varphi}=\mathbf{0}$, which means that $\tilde{\mathbf{p}}_{\text{opt}}=\mathbf{p}_0$. Obviously, the input needs to have at least $(Q+1)$ spectral tones, and this will enable identification of up to $2(Q+1)$ real-valued mismatch parameters. As the input spectrum becomes richer, we are more likely to have at least $(Q+1)$ independent rows, guaranteeing unique parameter identification. For theoretical purpose, we consider the following assumption: *The TIADC input has at least $(Q+1)$ distinct spectral tones at ω_n's, such that only one of $S_y^{0}(\omega_n)$ or $S_y^{0}(\omega_n-\omega_s/2)$ is nonzero*. Under this minimal asymmetric tone (MAT) assumption, (17) simplifies to

$$\begin{aligned}\mathbf{V}\mathbf{e_g}&=\mathbf{0},\\\mathbf{V}\mathbf{e_\varphi}&=\mathbf{0},\end{aligned} \tag{19}$$

where $\mathbf{V}$ is now a diagonally weighted vandermonde matrix,

$$\left[\mathbf{V}\right]_{n,m}=S_y^{0}(\omega_n)\omega_n^m. \tag{20}$$

$\mathbf{V}$ is nonsingular if and only if ω_n's are distinct. Therefore, the MAT condition strictly guarantees unique mismatch identification. The MAT condition is met if the input spectrum has a small unoccupied region not in a mirror symmetry across $f=\frac{1}{4}f_s$. Since the probability of $\mathbf{W}$ being singular has zero measure, $\mathbf{W}$ will be almost always nonsingular even if MAT is not met, as long as the input spectrum is rich enough.

Minimization of (13) can be realized in many different ways, although we discussed only its theoretical aspect due to page limitation. For example, if given enough computational power, exhaustive search can be performed over a single batch of data. Otherwise, gradual descent to the minimum over multiple batches may also be attempted with reduced computational cost (but with slower convergence). Depending on the implementation, observation of either corrected or uncorrected output may be more convenient than the other ($y[n]$ or $y'[n]$ in Fig.1 (c), respectively).

5. SIMULATION RESULTS

In this section, representative MATLAB simulation examples are given to demonstrate the proposed general mismatch correction.

The $M=2$ TIADC under simulation has 12-bit resolution, and each channel has a single pole around $0.6\omega_s$. Mismatch parameters are: 3% static gain error, 0.6% sampling time error and 2% pole location mismatch. The input signal has three equal-magnitude tones at $0.065\omega_s$, $0.185\omega_s$ and $0.405\omega_s$. It is readily seen that MAT is satisfied with Q up to 2. A single batch of 100,000 uncorrected

output samples is first acquired. Its cyclic autocorrelation is computed by time-averaging and then passed to minimization routine. The minimizer first computes 61-tap correction filters using (5) with the current mismatch estimation. Double convolution with correction filters is then performed upon the uncorrected cyclic autocorrelation to obtain R_y^{α}, the cyclic correlation of corrected output. Finally, the norm of $R_y^{I/2}$ is compared with the previous one (U_{max}=10) and parameter estimation is correspondingly updated, completing a single iteration. Built-in MATLAB searcher is used for parameter update.

Two representative mismatch models are tested for comparison: conventional gain-timing model and 2nd-order polynomial model (Q=2). Fig.2 (a) and (b) each compares the true CTF and its estimation with either mismatch model. Dotted lines are true magnitude and phase response, where the curvature is due to the pole location mismatch. Solid lines correspond to the best estimation, which is also the best fit to the true responses weighted by the input spectral density. 2nd-order modeling gives a good match, and the limitation of gain-timing model is clear. Mismatch-limited SNR is closely approximated by $1/|\tilde{H}(\omega)-H(\omega)|$ which is plotted in Fig.2 (c). Up to 35dB of improvement is observed as a direct result of generalized mismatch modeling.

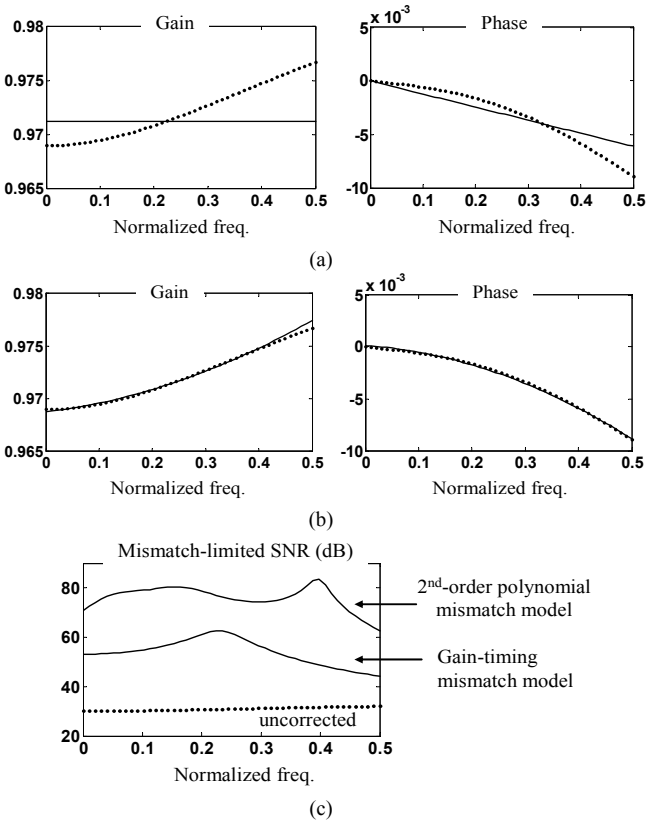

Figure 2. Calibration results from MATLAB runs. (a) Actual and estimated CTF using gain-timing model and (b) 2nd-order polynomial model (Dotted line: actual CTF response, solid line: estimated CTF response). (c) comparison of SNR level after calibration using each mismatch model

8. CONCLUDING REMARK

We have demonstrated that generalized mismatch errors can be blindly identified and corrected, achieving significant SNR and SFDR improvement (15~35dB), for an M=2 TIADC under realistic assumptions. Parameterized filter banks and cyclostationary spectral analysis is a key to the algorithm implementation and theoretical analysis, respectively.

Polynomial approximation in polar coordinate has been used for the present study, but in principle other parameterizations are also possible. The best parameterization will be application specific: It will capture the physics of mismatches with a minimal number of parameters while systematically avoiding the possibility of false correction. Although we focused on A/D conversion system, the proposed approach and theoretical framework can also be applied to general sampling networks where the sampler performance is sensitive to periodic patterning artifacts.

11. REFERENCES

[1] W. C. Black, Jr. and D. A. Hodges, "Time interleaved converter arrays," *IEEE J. Solid-State Circuits*, vol. SC-15, no. 6, pp. 1022-1029, Dec. 1980.

[2] J. Elbornsson, F. Gustafsson, and J.-E. Eklund, "Blind adaptive equalization of mismatch errors in a time-interleaved A/D converter system," *IEEE Trans. Circuits and Systems – I: Regular Papers*, vol. 51, No. 1, pp. 151-158, Jan. 2004.

[3] S. M. Jamal, D. Fu, M. P. Singh, P. J. Hurst, and S. H. Lewis, "Calibration of sample-time error in a two-channel time-interleaved analog-to-digital converter," *IEEE Trans. Circuits and Systems – I: Regular papers*, vol. 51, no. 1, pp. 130-139, Jan. 2004.

[4] V. Divi and G. Wornell, "Signal recovery in time-interleaved analog-to-digital converters," in *Proc. IEEE ICASSP*, vol. 2, pp. 593-596, May 2004.

[5] M. Seo, M. Rodwell, and U. Madhow, "Comprehensive digital correction of mismatch errors for a 400-MSamples/S, 80-dB SFDR time-interleaved analog-to-digital converter," *IEEE Trans. Microwave Theory Tech.*, vol. 53, no. 3, pp. 1072-1082, Mar. 2005.

[6] M. Seo, M. Rodwell, and U. Madhow, "Blind correction of gain and timing mismatches for a two-channel time-interleaved analog-to-digital converter," *39th Asilomar Conference on Signals, Systems, and Computers*, pp. 1121-1125, Oct. 2005.

[7] M. Seo, M. Rodwell, and U. Madhow, "Blind correction of gain and timing mismatches for a two-channel time-interleaved analog-to-digital converter: Experimental Verification," *IEEE Int'l Symp. Circuits and Systems,* Greece, pp. 3394-3397, May 2006.

[8] P. P. Vaidyanathan, *Multirate Systems and Filter Banks*, Englewood Cliffs, NJ: Prentice-Hall, 1993

[9] S. Ohno, and H. Sakai, "Optimization of filter banks using cyclostationary spectral analysis," *IEEE Trans. Signal Processing*, vol. 44, no. 11, pp. 2718-2725, Nov. 1996.